Case Studies in Construction Materials 16 (2022) e00809

Contents lists available at ScienceDirect

Case Studies in Construction Materials

journal homepage: www.elsevier.com/locate/cscm

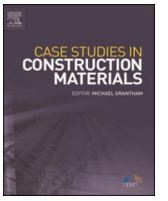

Case study

Evaluation of exhumed HDPE geomembranes used as a liner in Brazilian shrimp farming ponds

Fernando Luiz Lavoie [a,b,*], Marcelo Kobelnik [b], Clever Aparecido Valentin [b], Érica Fernanda da Silva Tirelli [a], Maria de Lurdes Lopes [c], Jefferson Lins da Silva [b]

[a] Department of Civil Engineering, Mauá Institute of Technology, São Caetano do Sul 09580–900, Brazil
[b] São Carlos School of Engineering, University of São Paulo-USP, São Paulo 13566–590, Brazil
[c] CONSTRUCT-GEO, Department of Civil Engineering, University of Porto; Porto 4200–465, Portugal

ARTICLE INFO

Keywords:
Geomembrane
HDPE
Shrimp farming ponds
TG
DSC
DMA

ABSTRACT

The present work evaluated three high-density polyethylene (HDPE) geomembranes exhumed from two shrimp farming ponds in the northeast of Brazil with nominal thicknesses of 0.8 mm. The CAM sample was exhumed from the bottom liner, and the CAM1 sample was exhumed from the slope liner, both after 8.25 years of field exposure in the same pond. The third sample, called CAM2, was exhumed from another shrimp farming pond after 3.0 years of service. It can be observed that the environmental exposure changed the CAM1 sample's behavior compared to the CAM sample. Changes in viscosity, stress cracking, and polymer unprotection by the antioxidants demonstrated that the environmental exposure in the field changed the initial conditions of the CAM1 sample. The CAM2 sample presented a high-density value, brittle tensile behavior, and a different thermal behavior from the other samples, as observed by the thermogravimetry (TG). Moreover, the CAM2 sample showed an event in dynamic mechanical analysis (DMA) presenting a significant decrease in stiffness. The first heating of differential scanning calorimetry (DSC) analysis showed an event before the melting points for all samples analyzed. Finally, the application of CAM1 and CAM2 samples as a liner can cause a system failure.

1. Introduction

Geomembranes are flexible polymeric sheets manufactured with smooth or textured faces and can be used in environmental applications, such as solid waste landfills, industrial waste, water ponds, waste liquid ponds, farm ponds, raised or buried water tanks, adduction and irrigation canals, pools and artificial beaches [1,2]. High-density polyethylene (HDPE) geomembrane presents high strength, good chemical compatibility, as well as a low cost. HDPE geomembranes have advanced since the 1980 s for landfill applications and they are currently the main geomembrane used as a liner in geotechnical facilities [3,4].

High-density polyethylene geomembranes have several different degradation mechanisms, but, for base-liner applications, oxidative degradation can be considered the most harmful [5]. The main process for HDPE oxidation is a free radical chain mechanism that occurs in two cycles. The first cycle is a chain reaction of alkyl/alkylperoxyl and the second cycle is the formation of new radicals by a chain reaction (homolysis of hydroperoxides). The oxidation can be stopped if all the links are foreclosed [6–8].

* Corresponding author at: Department of Civil Engineering, Mauá Institute of Technology, São Caetano do Sul 09580–900, Brazil.
E-mail addresses: fernando.lavoie@maua.br (F.L. Lavoie), mkobelnik@gmail.com (M. Kobelnik), cclever@sc.usp.br (C.A. Valentin), erica.tirelli@maua.br (É.F. da Silva Tirelli), lcosta@fe.up.pt (M. de Lurdes Lopes), jefferson@sc.usp.br (J.L. da Silva).

https://doi.org/10.1016/j.cscm.2021.e00809
Received 15 September 2021; Received in revised form 26 October 2021; Accepted 22 November 2021
Available online 23 November 2021

The oxidation of HDPE geomembranes can be evaluated through three different stages. The first stage is related to antioxidant depletion, which can be measured by the oxidative-induction time (OIT) test. In the second stage, the chain reaction begins, and changes in the molecular composition start. The third stage shows significant changes in the molecular composition with the formation of free radicals, and cross-linking occurs in the free radicals. The result of these changes is a completely changed molecular structure, a decrease in strength properties, the appearance of cracks, and there is an increase in the stress cracking susceptibility, culminating at the end of the service life [6,9,10].

Geomembranes manufactured using high-density polyethylene have been formulated since the 1990 s by additives such as carbon black (2–3%), antioxidants (> 0.5%), and resin (96–97.5%) [1,11,12]. Geosynthetics, similar to geomembranes in different applications, need to have a service lifetime of 30 years to 100 years [9].

Rowe et al. [13] examined the effect of physical aging on stress crack resistance (SCR) reduction before initiating oxidative degradation of eleven HDPE geomembranes. The authors used the notched constant load test (NCTL) to understand the effect of physical aging on the reduction of SCR. The samples were incubated in six different leachates for 116 months. A stress crack resistance value reduction was noted for a 1.5 mm-thick HDPE geomembrane after 3 months of incubation and stabilized until 116 months. According to the authors, there was no evidence of oxidative degradation after 3 months of incubation for ten out of eleven evaluated HDPE geomembrane samples. The mean reduction in SCR observed in this research for HDPE geomembranes immersed in leachate fluid was 37%.

Hsuan [14] investigated sixteen field construction works with stress cracking occurrences in HDPE geomembranes. According to the author, UV radiation and thermal exposure are involved in these various field issues about stress cracking reported in the US and Canada. The cracks formed in the geomembrane panels occurred or began in the seams and lasted to the panels.

Rowe and Shoaib [15] evaluated four HDPE geomembrane samples (1.5 mm of thickness) immersed in a brine solution with pH of 8.7 for 4 years at different temperatures (40–85 °C). The authors noted that physical degradation started before the total antioxidant depletion. Moreover, using the stress cracking resistance to understand the samples' durability in brine solution, it was observed that in samples with high resistance to initial stress cracking, the losses after incubation were greater than 50% of the initial value.

Geomembranes are generally welded in the field. The seam is considered a critical point for possible injuries and future leaks in the barrier system. Rollin et al. [16] reported that the total number of faults in geomembranes occurred in landfills, ponds and basins, and 55% of them were found at the seams. Stark et al. [17] evaluated seams made by industry and in the field of a polyolefin geomembrane (polypropylene) for a water reservoir project. According to the authors, the seams made by industry can minimize dirt and moisture in the seam, ambient temperature changes and wind. After good statistical data work, the results of this research showed that the seams made by industry were 9% stronger than field seams for peel strength and 10% stronger for shear strength. Moreover, seams according to industry data showed less variability.

Lavoie et al. [18] evaluated two different HDPE geomembrane samples exhumed from a municipal landfill leachate pond (2.0 mm thick and 5.17-year-old) and a sewage treatment aeration pond (1.0 mm thick and 2.75-year-old). The authors conducted thermal, physical and mechanical analyses. The thermogravimetric analyses (TG) showed an altered decomposition behavior for the landfill leachate pond sample, probably caused by the interaction with the leachate. The sewage pond sample presented low stress cracking resistance and low tensile elongation at break, compatible with the dynamic mechanic analysis (DMA), which showed an increase in the stiffness.

Ewais and Rowe [19] studied an HDPE geomembrane with 1.0 mm of the thickness of about five years immersed in synthetic leachate at different temperatures (25–95 °C) and in air and water at 55 °C. The authors observed changes in the sample's stress crack resistance (SCR) values before chemical degradation and before antioxidant depletion for temperatures lower than 70 °C. The major SCR value decrease was noted for the sample immersed in leachate at 55 °C, reaching 26% of the SCR value of the virgin sample. This behavior was attributed to morphological changes during aging that affected the interlamellar connections due to the annealing that increased the strength of the inter-lamellar connections and the proposed chain disentanglement mechanism.

HDPE geomembranes are often utilized as a flow barrier in landfills, mining facilities, canals, waste liquid ponds, and farm ponds. This research evaluated three exhumed high-density polyethylene (HDPE) geomembrane samples from two different shrimp farming ponds after 8.25 years of field exposure for the first pond and 3.0 years of field exposure for the second pond. Thermoanalytical and physical analyses were used to understand the final conditions of the HDPE geomembrane samples. Analyses such as thickness, density, carbon black content, melt flow index (MFI), tensile properties, stress crack resistance, oxidative-induction time (OIT), thermogravimetry (TG), differential scanning calorimetry (DSC), and dynamic mechanical analysis (DMA) were performed. Using an HDPE geomembrane as a liner of a shrimp farming pond is limited to some places globally, such as the northeast region of Brazil. This work aims to provide new data on the HDPE geomembrane performance in shrimp farming pond applications.

2. Materials and methods

2.1. Materials

This work evaluated three high-density polyethylene (HDPE) geomembrane samples exhumed from two different shrimp farming ponds in the northeast of Brazil with 0.8 mm of nominal thicknesses. The samples called "CAM" and "CAM1″ represent the same geomembrane installed in a shrimp farming pond and were collected after 8.25 years of field exposure. The CAM sample was exhumed from the bottom liner and had been in contact with the salinized water. The CAM1 sample was exhumed from the same pond as the CAM sample, but it was taken from the slope liner and had been in contact for 8.25 years with environmental conditions. The third sample (CAM2) was exhumed from another shrimp farming pond after 3.0 years of service. This pond has the particularity of being

Fig. 1. Shrimp farming pond representing the CAM and CAM1 samples.

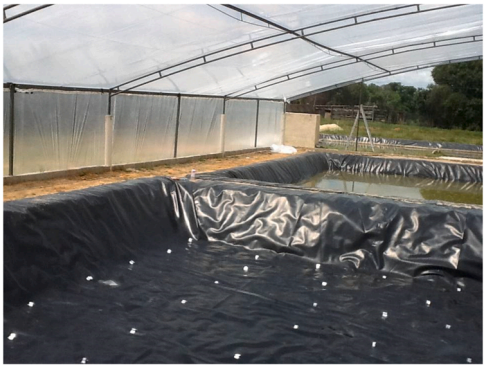

Fig. 2. Shrimp farming pond representing the CAM2 sample.

Table 1
Salinized water parameters used for shrimp cultivation [20].

Parameter	Average Value (8% of Salinization)	Average Value (16% of Salinization)
Dissolved Oxygen (mg/L)	5.81	5.49
Saturated Oxygen (%)	85.13	80.22
Water Temperature (°C)	27.81	27.54
pH	7.76	7.67
Total Alkalinity (mg $CaCO_3$/L)	93.69	120.06

covered with an agricultural plastic film. Figs. 1 and 2 show, respectively, the shrimp farming pond representing the CAM and CAM1 samples and the shrimp farming pond representing the CAM2 sample. Table 1 presents the salinized water parameters used for shrimp cultivation.

2.2. Physical properties

Physical analyses were performed in this research to understand the final conditions of the exhumed HDPE geomembrane samples. The thickness [21] was determined using a dead-weight loading gauge of 200 ± 0.2 kPa to measure the difference between the specimen and the reference (precision of 0.001 mm). The density of the samples [22] was determined by measuring the mass of the immersion sample of 1.0 ± 0.1 g (in a beaker with isopropyl alcohol at 21 ± 0.1 °C) with an analytical balance of a 0.0001 g of precision. The carbon black content [23] was determined using a muffle furnace at 605 ± 5 °C and an analytical balance with a precision of 0.0001 mm to measure the sample before and after burning. The melt flow index [24] was performed using a plastometer (with a smooth bore of 2.095 ± 0.005 mm in diameter and 8.000 ± 0.025 mm long) to extrude the material with a dead-weight load of 5 ± 0.01 kg at 190 ± 0.08 °C for 10 ± 0.01 min. The mass was determined with an analytical balance with a 0.0001 g of precision.

The oxidative-induction time (OIT) was determined using DSC equipment, model Q20, manufactured by TA Instruments, in New Castle, USA, using the standard test [25] at 200 ± 2 °C with a constant oxygen pressure of 140 ± 5 kPa, a heating rate of 20 ± 1 °C min^{-1} and flow rate of 50 ± 5 mL min^{-1}, and using the high-pressure test [26] at 150 ± 0.5 °C with a constant oxygen pressure of 3.4 ± 0.06 MPa and a heating rate of 20 ± 1 °C min^{-1}. The sample mass of 5 ± 0.5 mg in an aluminum crucible was used in both tests.

Tensile properties [27] were determined using a universal machine manufactured by EMIC in São José dos Pinhais, Brazil, model

DL 3000, with a 2-kN load cell, a test speed of 50 ± 1 mm min^{-1} and the IV dog bone specimen. The stress crack resistance [28] of the exhumed HDPE geomembrane samples analyzed in this work was performed using equipment manufactured by WT Indústria in São Carlos, Brazil, applying 30% of the sample's yield strength with 10 g of precision. The specimens were notched with 20% of the specimens' thicknesses (with 0.001 mm of precision) and immersed in a chemical solution (10 ± 0.1% of Igepal CO 630 and 90 ± 0.1% water) at 50 ± 1 °C. The rupture times of the specimens were recorded as a test result (with 1 s of precision).

2.3. Thermoanalytical methodology

Thermogravimetric analysis (TG) was conducted using a heating rate of 10 ± 1 °C min^{-1} under nitrogen purge gas with a flow rate of 90 ± 5 mL min^{-1}. The equipment used in this analysis was the Q50, manufactured by TA Instruments, in New Castle, USA.

The DSC analysis carried out in this study used the Q20 model, manufactured by TA Instruments, in New Castle, USA. The analysis was performed using a heating rate of 10 ± 1 °C min^{-1}, a temperature range of 25–200 ± 2 °C, nitrogen gas environment with a flow of 50 ± 5 mL min^{-1} and an aluminum crucible.

The DMA analysis was performed in the dual cantilever mode, with 10 ± 1 °C min^{-1} of heating rate, and heating from – 100 ± 2 °C to 130 ± 2 °C. The oscillation amplitude of 20 μm was used with a frequency of 1 Hz. The specimen's dimensions were 13 ± 1 × 35 ± 1 mm. The equipment used in this analysis was a Q800 equipment manufactured by TA Instruments, in New Castle, USA.

3. Results and discussion

3.1. Physical results

Tables 2 and 3 show the physical results of the HDPE geomembranes' exhumed samples compared to the minimum values of the GRI-GM13 [29], which is a standard specification of the minimum required values for HDPE geomembrane properties. This standard is used by manufacturers to carry out the quality control of manufacturing this product.

The CAM1 and CAM2 samples had mean thickness values lower than the nominal value, which can contribute to the premature degradation of these geomembranes as the thickness of the geomembrane influences the mechanical properties and the durability of the product [30]. After 8.25 years, the shrimp farming pond samples obtained density values near 0.940 g cm^{-3}. However, the CAM2 exhumed sample from another shrimp farming pond presented a higher density value of 0.952 g cm^{-3} than the minimum value of the GRI-GM13 [29]. This density value is considered high for a modern HDPE geomembrane. The high density of the CAM2 sample can be attributed to physical aging, which affected the crystallinity of the geomembrane. The DSC curve for this sample showed a different behavior in the melting point compared to that of the other samples. The carbon black content measured from the three samples was satisfactory, although the CAM1 sample presented a higher value than 3.0%.

The results of the melt flow index test showed an atypical behavior for the CAM1 sample. It was not possible to perform the test at the standard temperature (190 °C), as the material melted quickly. The test was then carried out at 160 °C, and the result of the melt flow index obtained was high (3.9939 g 10 min^{-1}). Different molecular changes of the polymer occurred among the samples from the

Table 2
Results of physical test of the exhumed HDPE geomembrane samples.

Samples	Thickness (mm)	Density (g cm^{-3})	CBC (%)	MFI (g 10 min^{-1})
CAM	0.800	0.937	3.03	1.4191
	(± 0.014)	(± 0.002)	(± 0.27)	(± 0.0325)
CAM1	0.769	0.941	3.14	3.9939[a]
	(± 0.011)	(± 0.004)	(± 0.45)	(± 0.2188)
CAM2	0.772	0.952	2.75	0.5831
	(± 0.038)	(± 0.002)	(± 0.52)	(± 0.1380)
GRI-GM13[29]	≥ 0.80	≥ 0.940	2.0–3.0	–

Standard deviations are between brackets.
[a] Test carried out at 160 °C.

Table 3
Results of physical test of the exhumed HDPE geomembrane samples.

Samples	Std. OIT (min)	HP OIT (min)	Tens. break resistance (kN m^{-1})	Tens. break elongation (%)	SCR (h)
CAM	6.36	60.60	19.23	684.63	1151.98
	(± 0.52)	(± 4.81)	(± 3.11)	(± 96.46)	(± 44.64)
CAM1	9.65	0	16.12	627.07	4.25
	(± 0.70)	(± 0)	(± 2.09)	(± 63.27)	(± 1.52)
CAM2	67.61	166.05	16.37	312.74	90.41
	(± 5.13)	(± 15.06)	(± 2.15)	(± 335.42)	(± 17.01)
GRI-GM13[29]	≥ 100	≥ 400	≥ 22	≥ 700	≥ 500

Standard deviations are between brackets.

shrimp farming pond after 8.25 years of exposure, considering that the CAM and CAM1 samples represent the same geomembrane; the first sample exhumed from the bottom liner and the other sample exhumed from the slope liner. The CAM2 sample presented a typical melt flow index test result.

The CAM and CAM1 samples showed a tendency to decrease the ductile tensile, although the tensile resistance at the break mean value and the tensile elongation at the break mean value were lower than the minimum required values prescribed by the GRI-GM13 [29]. The CAM2 sample presented a brittle behavior. The average tensile elongation value of this sample was lower than 350%. It means less than 50% of the minimum required for the GRI-GM13 [29] for the tensile elongation value.

The difference between the stress crack resistance results of the CAM and CAM1 samples was evident. The CAM sample (exhumed from the bottom liner of the pond) presented a high-stress crack resistance, higher than the minimum required value by GRI-GM13 [29]. Moreover, the CAM1 sample (exhumed from the pond's slope liner) presented a low-stress crack resistance near zero. An HDPE geomembrane with a low melt flow index value can denote a polymer with a high molecular weight that provides a high SCR [31]. It can be observed which CAM1 sample had a high MFI test result and a low SCR test result. CAM2 sample presented a lower value than the minimum required value by GRI-GM13 [29].

Antioxidant depletion was measured using the Std. OIT and the HP OIT tests, including the analyses of different antioxidant groups. The results of the CAM1 sample showed total antioxidant depletion for the HP OIT test and almost total antioxidant depletion for the Std. OIT test, demonstrating unprotection of the additives to the polymer against the thermo-oxidative degradation. The CAM sample still showed some antioxidant amount for the HP OIT test but had a low Std. OIT value. The CAM2 sample presented OIT values lower than the minimum required values by the GRI-GM13 [29].

3.2. Thermoanalytical evaluation

Fig. 3 shows the TG/DTG curves for the CAM, CAM1 and CAM2 samples. It can be observed that the CAM and CAM1 samples have similar thermal behavior, while the CAM2 sample, which was collected from a shrimp farming pond after 3 years of service, shows noticeably different behavior. As mentioned, the CAM2 sample was exhumed from an area protected directly from the sunlight. It is interesting to observe that for all these samples, there is thermal stability up to a temperature of 248 °C.

For the CAM2 sample, the first thermal decomposition step occurs from 248 to 396 ºC, with a total loss in this range of 10.46%, as seen in the DTG curve. The second stage of thermal decomposition occurs between 396 ºC and 427 ºC, with a mass loss of 55.21%, which shows a single stage, as seen in the DTG curve. The third and fourth stages occur in the intervals of 427 – 490 ºC and 490 – 605 ºC, and show mass variations of 24.87% and 8.19%, respectively.

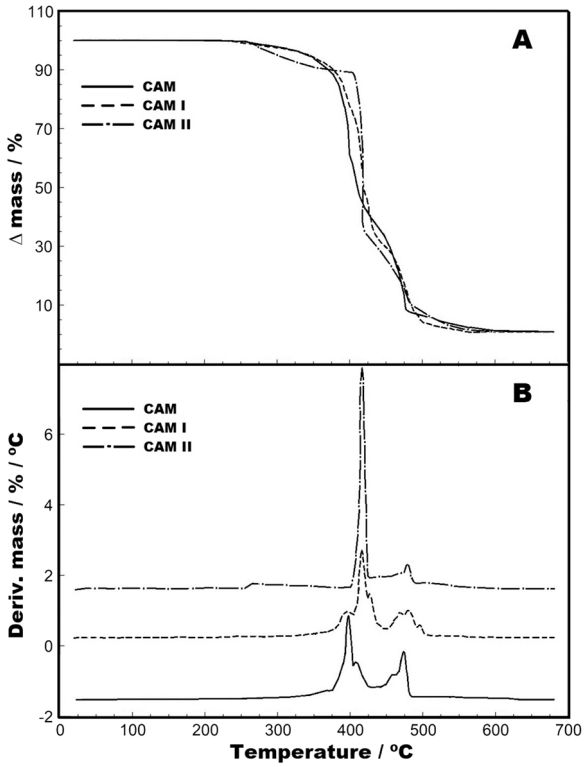

Fig. 3. TG/DTG curves for the samples, CAM sample (solid line), CAM1 sample (dashed line), and CAM2 sample (dotted line) under nitrogen purge gas with a flow up to 90 mL min^{-1}, using 10 °C min^{-1} as heating rate. (A) Samples' TG curves. (B) Samples' DTG curves.

The CAM and CAM1 samples (Fig. 3A and B) have similar thermal behavior up to a temperature of 347 ºC. However, they show different behavior after that in the TG/DTG curves. The CAM sample, which was underwater throughout the entire service time, presented a higher thermal decomposition than the other two samples, while the CAM1 sample, exposed to UV radiation at the pond's slope shows a slightly smaller decomposition. This effect is attributed to the different conditions in which both materials were found. Mass variations are best observed in the DTG curves, where it can be observed that the CAM and CAM1 samples have five main ranges of mass variation. For the CAM sample, the loss and temperature ranges are as follows: 5.27% (235–349 °C), 5.40% (349–381 °C), 16.18% (381–408 °C), 43.34% (408–451 °C) and 28.75% (451–590 °C). The CAM1 sample shows the following mass losses and respective temperature ranges: 5.83% (235–349 °C), 7.51% (349–381 °C), 28.67% (381–403 °C), 24.67% (403–448 °C), 31.58% (448–590 °C).

The DSC curves are shown in Fig. 4. Three analysis conditions can be observed: (A) first heating, (B) second heating, and (C) cooling (after the first heating).

The first heating (Fig. 4A) shows the melting point of the samples in the conditions under which they were collected in the respective ponds and locations. Note that all samples have a melting peak at a temperature of 126 °C. Before the melting point, there were baseline change events between 75 and 90 °C for the CAM sample, 90–102 °C for CAM1, and 71–82 °C for the CAM2 sample. Moreover, the melting peak of the CAM2 sample shows a shoulder, which is not seen in the other samples. Valentin et al. [32] performed the DSC characterization of HDPE geomembrane samples of different thicknesses and manufacturers. The events observed before and during melting in the samples in this work were also observed events that shifted the baseline and the presence of shoulders as the one seen here. Furthermore, Fig. 4B shows the second heating of these materials. It can be observed that in all of the samples, the events observed in the first heating disappear because, with the heating, the molecular history disappeared due to the formation of a

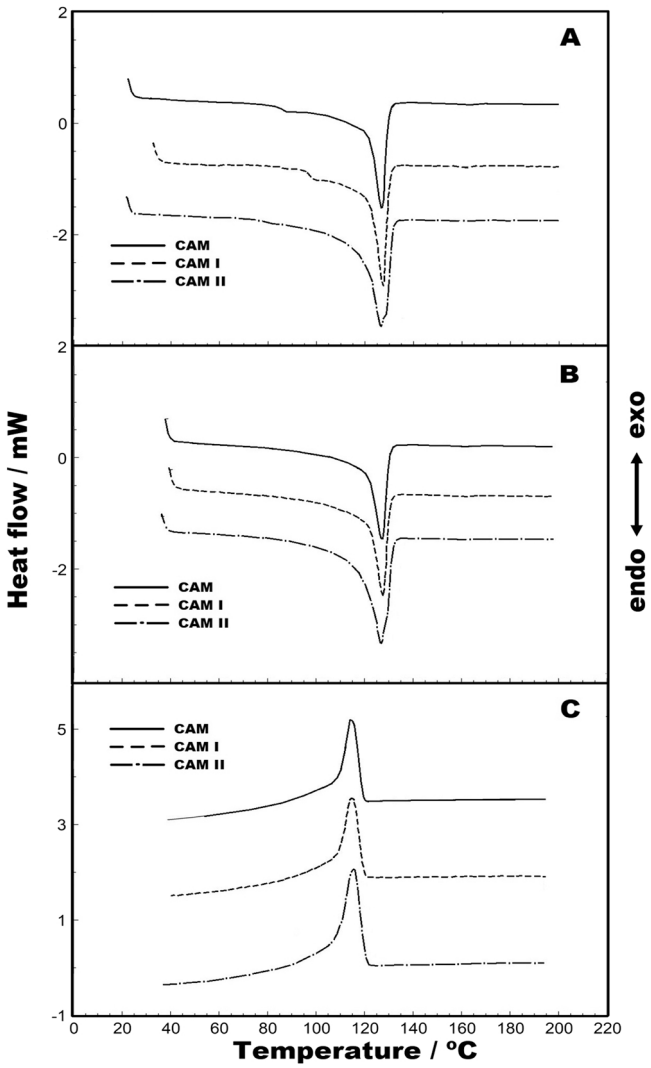

Fig. 4. DSC curves for the samples, CAM sample (solid line), CAM1 sample (dashed line), and CAM2 sample (dotted line) under nitrogen purge gas with a flow up to 50 mL min^{-1}, using 10 °C min^{-1} as heating rate. (A) First heating. (B) Second heating. (C) cooling (after the first heating).

homogeneous material. This fact shows that the use of the melting point for quality control analysis is not adequate, as the molecular relaxation of the polymer causes melting events. However, it should be noted that the evaluation of the melting point of pure substances presents sharper peaks in DSC curves, and the presence of impurity can be detected or evaluated by the peak area. As HDPE polymers are not pure but with different additives, melting peaks are not suitable for evaluation via DSC [33]. Fig. 4C shows the crystallization peaks, which are obtained after the first heating. It can be observed that the crystallization peaks are coincident (115 °C), attributed to the effect caused by the fusion (homogenization of the material).

The results obtained from the DMA analyses are shown in Fig. 4. In the literature, the studies and the DMA results focus on three main concepts: storage modulus, loss modulus, and viscoelastic material information (tan delta), which are calculated from the material's response to the sine wave [34,35].

Variations in the storage modulus (Fig. 5A) show the degree of crosslinking in the materials' molecules. At low temperatures, the polymer has a rigid behavior, while at high temperatures, the stiffness decreases. Thus, it can be observed that the CAM and CAM1 samples presented similar behaviors. In contrast, the CAM2 sample presents an event between − 44 and 32 ºC, which shows a significant decrease in stiffness. After 32 ºC, there is a decrease in the storage modulus, attributed to the increase in the materials' viscoelastic behavior. The evaluation of loss modulus (Fig. 5B) can succinctly be attributed to the energy loss due to the polymer's molecular vibrations. The molecular vibration causes heat loss. In this case, it can be understood that the CAM and CAM1 samples presented similar behavior. Finally, the evaluation of tan delta, seen in Fig. 5C, presents a continuous increase, which shows information about the materials' viscoelastic behavior because it is a relationship between the loss and storage modulus. An increase in temperature causes the polymeric material to absorb energy and tends to molecular disassembly, which effectively occurs at the melting point, where the material has a viscous behavior.

Valentin et al. [32] evaluated virgin samples of different HDPE geomembranes, and no changes were observed in the performed analyses. Therefore, the material's exposure in construction work changes the initial conditions of the polymer [35].

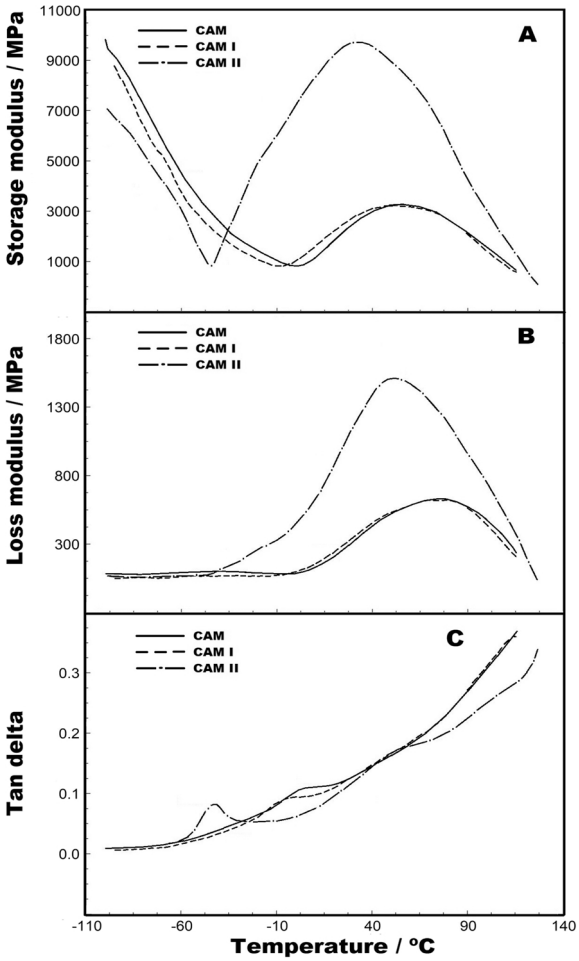

Fig. 5. DMA curves for the samples, CAM sample (solid line), CAM1 sample (dashed line), and CAM2 sample (dotted line) using 10 °C·min^{-1} as heating rate. (A) Storage modulus. (B) Loss modulus. (C) Tan delta.

4. Conclusions

This work evaluated three HDPE geomembrane samples exhumed from two shrimp farming ponds using physical and thermal analyses.

The high density of the CAM2 sample can be attributed to physical aging, which affected the crystallinity of the geomembrane. The DSC curve for this sample showed a different behavior in the melting point compared to the other samples. The CAM1 sample presented an atypical MFI result because the result was high, and the material melted quickly. This behavior showed that polymer molecular changes occurred in this sample.

The CAM2 sample presented a brittle tensile behavior, with the tensile elongation at the break mean value less than 50% of the minimum required for the GRI-GM13. The CAM and CAM1 samples showed a tendency to decrease the ductile behavior.

The results of the stress crack resistance for the CAM and CAM1 samples showed a different behavior between the samples. The CAM sample presented a high value of stress crack resistance; however, the CAM1 sample presented a low-stress crack resistance near zero. It can be observed which CAM1 sample showed a high MFI test and a low SCR test, demonstrating the effect of weather exposure on this sample.

The OIT test results for the CAM1 sample demonstrated the unprotection from the additives to the polymer against thermo-oxidative degradation after exposure.

The TG analysis showed a different thermal behavior for the CAM2 than the other samples analyzed. The CAM sample presented a higher thermal decomposition than the CAM1 sample. This effect is attributed to the different conditions in which the materials were found.

The first heating of the DSC analysis, which represents the samples' final conditions in the field, demonstrated events before the melting point, between 75 and 90 °C for the CAM sample, 90–102 °C for CAM1, and 71–82 °C for the CAM2 sample. Furthermore, the melting peak of the CAM2 sample shows a shoulder, which is not seen in the other samples.

The DMA analysis conducted for the samples showed that the CAM and CAM1 samples presented similar behaviors. Moreover, the CAM2 sample presents an event between − 44 and 32 ºC, which shows a significant decrease in stiffness. After 32 ºC, there is a decrease in the storage modulus, attributed to the increase in the materials' viscoelastic behavior.

Therefore, it was observed that the environmental exposure for 8.25 years changed the behavior of the CAM1 sample compared to the CAM sample. Changes in viscosity, stress crack resistance, and polymer protection by the antioxidants demonstrated that the environmental exposure in the field changed the initial conditions of the CAM1 sample. Moreover, the CAM2 sample presented a high-density value, brittle tensile behavior, and a different thermal behavior than the other samples. The CAM2 sample showed an event in the DMA analysis that presented a significant decrease in stiffness.

Finally, the CAM1 sample presented an atypical viscosity, low SCR result, unprotection from the additives against the oxidative degradation, certainly reaching the lifetime. The CAM2 sample showed a brittle tensile behavior, a low SCR value, and a low Std. OIT value and can culminate in a system failure. The CAM sample changed its physical and thermal behavior and could cause a liner rupture in the short term.

Declaration of Competing Interest

The authors declare that they have no known competing financial interests or personal relationships that could have appeared to influence the work reported in this paper.

References

[1] Vertematti J.C.: Manual Brasileiro de Geossintéticos. Blücher, São Paulo, 2015.
[2] Palmeira E.M.: Geossintéticos em Geotecnia e Meio Ambiente. Oficina de Textos, São Paulo, 2018.
[3] R.M. Koerner, Designing with Geosynthetics, Prentice Hall Publ. Co., New Jersey, Englewood Cliffs, 2005.
[4] J. Scheirs. A guide to Polymeric Geomembranes: a practical approach, 1st ed..,, Wiley, London, 2009.
[5] Y.G. Hsuan, R.M. Koerner, The single point-notched constant Tension load test: a quality control test for assessing stress crack resistance, Geosynth. Int. 2 (1995) 831–843, https://doi.org/10.1680/gein.2.0038.
[6] R.K. Rowe, H.P. Sangam, Durability of HDPE geomembranes, Geotext. Geomembr. 20 (2002) 77–95, https://doi.org/10.1016/S0266-1144(02)00005-5.
[7] T. Kelen. Polymer degradation, 1st ed..,, Van Nostrand Reinhold Co, New York, 1983.
[8] N. Grassie, G. Scott. Polymer degradation and stabilization, 1st ed..,, Cambridge University Press, New York, 1985.
[9] S.W. Perkins, in: R.W. Sarsby (Ed.), Geosynthetics in Civil Engineering, Woodhead Published Limited, Cambridge, 2007 cap. 2.
[10] F.B. Abdelaal, R.K. Rowe, Degradation of an HDPE geomembrane without HALS in chlorinated water, Geosynth. Int. 26 (2019) 354–370, https://doi.org/10.1680/jgein.19.00016.
[11] R.K. Rowe, A.M.R. Ewais, Ageing of exposed geomembranes at locations with different climatological conditions, Can. Geotech. J. 52 (2015) 326–343, https://doi.org/10.1139/cgj-2014-0131.
[12] Hsuan, Y.G.; Schroeder, H.F.; Rowe, R.K.; Müller, W.; Greenwood, J.; Cazzuffi, D.; and Koerner, R.M.: Long-term performance and lifetime prediction of geosynthetics. In Proceedings of the 4th European Conference on Geosynthetics, 2008, Edinburgh, September. Keynote paper.
[13] R.K. Rowe, M.S. Morsy, A.M.R. Ewais, Representative stress crack resistance of polyolefin geomembranes used in waste management, Waste Manag 100 (2019) 18–27, https://doi.org/10.1016/j.wasman.2019.08.028.
[14] Y.G. Hsuan, Data base of field incidents used to establish HDPE geomembrane stress crack resistance specifications, Geotext. Geomembr. 18 (2000) 1–22, https://doi.org/10.1016/S0266-1144(99)00018-7.
[15] R.K. Rowe, M. Shoaib, Effect of brine on long-term performance of four HDPE geomembranes, Geosynth. Int. 24 (2017) 508–523, https://doi.org/10.1680/jgein.17.00018.
[16] Rollin, A.L., Marcotte, M., Jacqueline, T., Chaput, L.: Leak location in exposed geomembrane liners using an electrical leak detection technique. In: Proceedings of Geosynthetic'99, vol. 2. Industrial Fabrics Association International, 1999, Boston, USA, IFAI, Roseville, MI, USA, pp. 615–626.

[17] T.D. Stark, M.A. Hernandez, D.S. Rohe, Geomembrane factory and field thermally welded seams comparison, Geotext. Geomembr. 48 (2020) 454–467, https://doi.org/10.1016/j.geotexmem.2020.02.004.
[18] F.L. Lavoie, C.A. Valentin, M. Kobelnik, J. Lins da Silva, M.L. Lopes, HDPE geomembranes for environmental protection: two case studies, Sustainability 12 (20) (2020) 8682, https://doi.org/10.3390/su12208682.
[19] A.M.R. Ewais, R.K. Rowe, Effect of aging on the stress crack resistance of an HDPE geomembrane, Polym. Degrad. Stab. 109 (2014) 194–208, https://doi.org/10.1016/j.polymdegradstab.2014.06.013.
[20] A.C.F. Spelta, Caracterização e Avaliação da Qualidade da Água de Sistema Intensivo de Produção de Camarão com Bioflocos em Diferentes Salinidades, Federal University of Minas Gerais, Brazil, 2016.
[21] ASTM (American Society for Testing and Materials). ASTM D 5199 Standard Test Methods for Measuring the Nominal Thickness of Geosynthetics; ASTM: West Conshohocken, PA, USA, 2019; p. 4.
[22] ASTM (American Society for Testing and Materials). ASTM D 792 Standard Test Methods for Density and Specific Gravity (Relative Density) of Plastics by Displacement; ASTM: West Conshohocken, PA, USA, 2020; p. 6.
[23] ASTM (American Society for Testing and Materials). ASTM D 4218 Standard Test Method for Determination of Carbon Black Content in Polyethylene Compounds by the Mue-Furnace Technique; ASTM: West Conshohocken, PA, USA, 2020; p. 4.
[24] ASTM (American Society for Testing and Materials). ASTM D 1238 Standard Test Methods for Melt Flow Rates of Thermoplastics by Extrusion Plastometer; ASTM: West Conshohocken, PA, USA, 2020; p. 16.
[25] ASTM (American Society for Testing and Materials). ASTM D 3895 Standard Test Method for Oxidative-Induction Time of Polyolefins by Differential Scanning Calorimetry; ASTM: West Conshohocken, PA, USA, 2019; p. 7.
[26] ASTM (American Society for Testing and Materials). ASTM D 5885 Standard Test Method for Oxidative Induction Time of Polyolefin Geosynthetics by High-Pressure Differential Scanning Calorimetry; ASTM: West Conshohocken, PA, USA, 2020; p. 5.
[27] ASTM (American Society for Testing and Materials). ASTM D 6693 Standard Test Methods for Determining Tensile Properties of Nonreinforced Polyethylene and Nonreinforced Flexible Polypropylene Geomembranes; ASTM: West Conshohocken, PA, USA, 2020; p. 5.
[28] ASTM (American Society for Testing and Materials). ASTM D 5397 Standard Test Method for Evaluation of Stress Crack Resistance of Polyolefin Geomembranes Using Notched Constant Tensile Load Test; ASTM: West Conshohocken, PA, USA, 2020; p. 7.
[29] GRI—GM13, Test methods, test properties and testing frequency for high density polyethylene (HDPE) smooth and textured geomembranes SM, Geosynthetic Institute, 2021.
[30] Islam, M.Z.; Rowe, R.K. Effect of HDPE geomembrane thickness on the depletion of antioxidants. In Proceedings of the 60th Canadian Geotechnical Conference and the 8th Joint CGS/IAH-CNC Groundwater Conference, Ottawa, ON, Canada, 21–24 October 2007.
[31] Y.G. Hsuan, Data base of field incidents used to establish HDPE geomembrane stress crack resistance specifications, Geotext. Geomembr. 18 (2000) 1–22, https://doi.org/10.1016/S0266-1144(99)00018-7.
[32] C.A. Valentin, J.L. Silva, M. Kobelnik, C.A. Ribeiro, Thermoanalytical and dynamic mechanical analysis of commercial geomembranes used for fluid retention of leaching in sanitary landfills, J. Anal. Calorim. 136 (2018) 471–481, https://doi.org/10.1007/s10973-018-7690-0.
[33] A. Ksiqczak, T. Ksiqczak, T. Zielenkiewicz, Influence of purity on the thermal stability of solid organic compounds, J. Anal. Calorim. 77 (2004) 233–242, https://doi.org/10.1023/B:JTAN.0000033208.42367.97.
[34] K.P. Menard, Dynamic Mechanical Analysis: A Practical Introduction, CRC Press, New York, 1999.
[35] H.A. Khonakdar, J. Morshedian, U. Wagenknecht, S.H. Jafari, An investigation of chemical crosslinking effect on properties of high-density polyethylene, Polym 44 (2003) 4301–4309, https://doi.org/10.1016/S0032-3861(03)00363-X.